AIAA Guidance, Navigation, and Control Conference and Exhibit
5-8 August 2002, Monterey, California

AIAA 2002-4774

AIAA-2002-4774

PERFORMANCE ANALYSIS OF NOMINAL SCHEME AND DECOUPLING LOOP SCHEME FOR RF SEEKER

Abhijit Bhattacharyya[1] & R.N.Bhattacharjee[2]

1. Scientist 'C' , Programme AD, DRDL Campus, P.O-Kanchanbagh, Hyderabad 500058, India, Email :abhijit689@yahoo.com
2 . Scientist 'F' , DRDL, P.O-Kanchanbagh, Hyderabad 500058, India

1. Abstract:

Airborne seeker has to perform the role of target tracking with low pointing error as well as good disturbance rejection particularly with respect to flight vehicle motion. Although seeker with high stabilization loop gain *(K_{sl})* performs the role of good disturbance rejection, it inherently increases the cost, weight and power requirements of the seeker. Good disturbance rejection is essential as disturbances in the form of high magnitude body rates has to be attenuated sufficiently so that its effect is as low as possible in the guidance signals to be tapped from the seeker. A special configuration known as **decoupling loop scheme** is sometimes employed to annul the effect of body rate disturbances in the synthesized LOS rate signal which is generally tapped from the seeker for guidance. Decoupling loop approach works well with IR / IIR seeker based homing guidance, but its effectiveness is not yet explored when a parasitic path exists in seeker in the form of radome aberration error as is the case in all RF seekers. The present paper deals with performance analysis of **decoupling loop scheme and nominal scheme** from the point of view of inner guidance loop (fig.1 and fig.2) stability and body rate decoupling from synthesized sight line rate in the presence of radome slope error. Generic formula of body rate decoupling from guidance signal; i.e synthesized sight line rate is derived in case of RF seeker for both nominal and decoupling loop scheme in the presence of radome slope error. The basic difference of both the schemes affecting seeker and guidance performance is brought out in a generic manner for different types of flight vehicles with varying response characteristics and different engagement situations. The stability of inner guidance loop of the two schemes, characterized by different realistic stabilization loop gains for different types of (fast or slow) flight vehicles, different engagement situations and guidance loop response time achievable in both the schemes are compared. The reported studies show that decoupling loop scheme shows good promise for RF seeker based terminal guidance with lower stabilization loop gain and for fast / moderately fast flight vehicle thereby saving on cost, weight and motor power, whereas for higher stabilization loop gain, advantages of decoupling scheme diminishes in both aspects of body rate decoupling and inner guidance loop stability. Thus, higher stabilization loop gain is required only for flight vehicles of slow basic response characteristics.

Symbols :

N'	Navigation Constant
V_c, V_m	Closing Velocity , Flight Vehicle Velocity
T_α	Incidence Lag of Flight Vehicle
R/r	Radome Slope error
$\dot{\theta}_t$	Kinematic Sight Line Rate
ε_t	Boresight error before signal processor
$K_{sp,}$	Seeker Signal Processor Gain
K_{sp}	Signal Processor Gain used for Decoupling
K_cG_c	Track Loop Gain and compensator
T_{seeker}	Ist order track loop time constant of seeker
δ_{sc}	Commanded Dish rate input to Stab. Loop
$KG(s)$	Stab. Loop Transfer Function of Seeker
K_{sl}	Stab. Loop gain of Seeker
$\dot{\theta}_{ib}$	Body rate of flight vehicle
$\hat{\dot{\theta}}_t$	Synthesized sight line rate for guidance
$\hat{\dot{\theta}}_{tn}, \hat{\dot{\theta}}_{td}$	Synthesized Sight Line Rate , Nominal & Decoupling Loop Scheme
ω_{icm}	Inertial Sight Line rate (Input to the Gyro)
$\dot{\theta}_g$	Gimbal Angle rate
T_{noise}	Noise Filter Time Constant
T_{ap}	Dominant mode time Constant of Autopilot
ω_{ap}' ξ_{ap}	Natural frequency, Damping ratio of nondominant 2[nd] order mode of Autopilot
ω_z	Nonminimum phase zero of flight vehicle
n_c	Commanded Acceleration to the Autopilot
n_L	Achieved Acceleration of the flight vehicle
$T_g(s)$	$T_{seeker}+T_{noise}+T_{ap}+2\xi_{ap}/\omega_{ap}$ (Guidance Time Constant)

2.Introduction :

For terminal guidance, a seeker is generally employed for target tracking with low pointing error. Seeker should have good disturbance rejection capability particularly with respect to low frequency body rate signals typically varying from 0.5 Hz to 5 Hz and magnitudes varying from low to high value depending on flight conditions and type of flight vehicle. This is required for synthesizing pure guidance signal from seeker measurements. This body rate disturbance rejection property is known as decoupling which is defined as the ratio $\left|\hat{\dot{\theta}}_t / \dot{\theta}_{ib}\right|$, i.e., gain attenuation of body rate component in the synthesized sight line rate signal used for guidance. The inner guidance loop of nominal seeker based guidance scheme is shown in fig.1. Seeker with sufficiently high stabilization loop gain provides good attenuation of body rate signal in the synthesized sight line rate $\hat{\dot{\theta}}_t$ [1]. In a nominal seeker based guidance scheme, the body rate decoupling as well as the inner guidance loop stability characteristics are already well established [3]. For almost annulling the body rate component in the guidance signal to a great extent, decoupling loop scheme (fig.2) can be one such effective scheme designed by the authors. This scheme improves body rate decoupling to a great extent and gives rise to higher margin of inner guidance loop stability in IR / IIR seeker based guidance scheme, thereby facilitating design of faster and accurate guidance. The effectiveness of this method is not yet explored in an RF seeker based guidance scheme.

In this paper, first generic relations of body rate decoupling of both nominal and decoupling loop scheme is carried out for any RF seeker. From this generic relations, simplified condition is analyzed and conclusion is arrived for body rate decoupling performance of both the schemes for different stabilization loop gain and radome slope error. Next, stability and performance characteristic of both schemes are examined and analyzed in detail for different combinations of RF seekers characterized by track loop time constant, stabilization loop gain, radome slope error and flight vehicles characterized by turning rate time constant, corresponding autopilot time constant and different engagement parameters including V_c/V_m ratio. Generic conclusions are then drawn regarding the two schemes catering and covering for large variations of seeker and flight vehicle parameters, engagement situations thereby covering different possible combinations of RF seekers and flight vehicles for seeker based guidance to a great extent.

3. Derivation of decoupling for nominal and decoupling loop scheme:

Decoupling of nominal seeker based guidance loop in the presence of radome slope error, can be shown to be

$$\frac{\hat{\dot{\theta}}_{tn}}{\dot{\theta}_{ib}} = \frac{-\left(1 + RKG\ (s)\right)}{\dfrac{s\left(1 + KG\ (s)\right)}{K_{sp} K_C G_C (s)} + (1 - R)KG\ (s)} \qquad (1)$$

If stabilization loop transfer function $KG\ (s)$ can be approximated as K_{sL}/s, (i.e., $KG\ (s) = K_{sL}/s$) and track loop can be approximated as a first order transfer function T_{seeker}, i.e., $K_{sp}K_C G_C\ (s) = 1/T_{seeker}$, then decoupling can be written as

$$\frac{\hat{\dot{\theta}}_{tn}}{\dot{\theta}_{ib}} = \frac{-\left(s + RK_{sL}\right)}{s^2 T_1 + sK_{sL}T_1 + (1-R)K_{sL}} \qquad (2)$$

$$= \frac{-RK_{sL}\left(1 + \dfrac{s}{RK_{sL}}\right)}{K_{sL}\left(\dfrac{s^2 T_1}{K_{sL}} + sT_1 + (1-R)\right)} \qquad (3)$$

$$\approx \frac{-R\left(1 + \dfrac{s}{RK_{sL}}\right)}{(1 + sT_1)\left(1 + \dfrac{s}{K_{sL}}\right)} \qquad \begin{pmatrix} \because |R| \to 0 \\ \because \dfrac{1}{K_{sL}} \langle\langle 1 \end{pmatrix} \qquad (4)$$

If $R = 0$,

$$\frac{\hat{\dot{\theta}}_{tn}}{\dot{\theta}_{ib}} \approx \frac{-s}{K_{sL}(1 + sT_1)\left(1 + \dfrac{s}{K_{sL}}\right)} \qquad (5)$$

In the absence of any radome slope error, equation 5 was already derived in [1] for simplified case only. Here the general expression of loop decoupling is shown for nominal scheme from which any simplified condition can be arrived at.

When decoupling loop scheme is employed, the expression of decoupling can be shown to be

$$\frac{\hat{\dot{\theta}}_{td}}{\dot{\theta}_{ib}} = \frac{-F(s)(1 + RKG(s)) + \dfrac{K'_{sp}}{K_{sp}}}{(1 + KG(s))\left(\dfrac{s}{K_{sp}K_C G_C(s)} + \dfrac{K'_{sp}}{K_{sp}}\right)} \qquad (6)$$

where,

$$F(s) = \frac{s + sKG(s) + K'_{sp}K_C G_C(s)KG(s)}{s + sKG(s) + (1-R)K_{sp}K_C G_C(s)KG(s)} \qquad (7)$$

In case of perfect loop decoupling, i.e., $K'_{sp} = K_{sp}$, decoupling can be written as

$$\therefore \frac{\hat{\dot{\theta}}_{td}}{\dot{\theta}_{ib}} = \frac{-\left((F(s) - 1) + RKG\ (s)\right)}{(1 + KG\ (s))\left(\dfrac{s}{K_{sp}K_C G_C\ (s)} + 1\right)} \qquad (8)$$

Radome slope error is generally close to 0, i.e, $/R/ \to 0$ and $\therefore K_{sp}' = K_{sp}$; $F(s) \approx 1$ from equation 7.

$\therefore$ Decoupling $\dfrac{\dot{\hat{\theta}}_{td}}{\dot{\theta}_{ib}}$ can be written as

$$\frac{\dot{\hat{\theta}}_{td}}{\dot{\theta}_{ib}} = \frac{-RKG(s)}{(1+KG(s))\left(\dfrac{s}{K_{sp}K_C G_C(s)}+1\right)} \tag{9}$$

As in nominal scheme, if stabilization loop transfer function $KG(s)$ can be approximated as K_{sL}/s, (i.e., $KG(s) = K_{sL}/s$) and track loop can be approximated as a first order transfer function with time constant T_{seeker}, i.e., $K_{sp}K_C G_C(s) = 1/T_{seeker}$, then track closed decoupling can be written as

$$\frac{\dot{\hat{\theta}}_{td}}{\dot{\theta}_{ib}} \approx \frac{-\dfrac{RK_{sL}}{s}}{\left(1+\dfrac{K_{sL}}{s}\right)(sT_{seeker}+1)}$$

$$= \frac{-R}{\left(1+\dfrac{s}{K_{sL}}\right)(1+sT_{seeker})} \tag{10}$$

4. Decoupling performance of RF Seeker (Nominal & Decoupling Loop Scheme):

With radome slope error being close to zero, for nominal scheme; loop decoupling depends on seeker stabilization and track loop parameters as is evident from equation 5. From equation 10, it is clear that when radome slope error is close to zero, decoupling scheme gives rise to very high attenuation of body rate coupling leading to very high decoupling and thus guidance loop can be made quite fast till maintaining inner guidance loop stability. This faster guidance particularly during end phase of homing when seeker noise is low leads to considerably lower miss distance. As radome slope error (R) increases, the body rate to synthesized LOS rate $\dot{\hat{\theta}}_t / \dot{\theta}_{ib}$ gain curve shifts upwards thereby reducing the decoupling ratio for both schemes. With realizable radome slope error values (For ex: $R = \pm 0.02$) ; comparison of body decoupling performance of both the schemes are investigated. With radome slope error $\neq 0$, zero at $-RK_{sl}$ and pole corresponding to first order seeker lag $(-1/T_{seeker})$ balances out for higher value of stabilization loop gain (say $K_{sl} = 600$ *etc*) in nominal scheme for positive R, and the gain attenuation effect of decoupling scheme is not significantly higher generally in the body frequency of interest upto 4 Hz. However; for lower K_{sl} (say of the order of 100), due to appreciably high gain amplification from low frequency zero at $-RK_{sl}$, gain increases with frequency till it is balanced out by the seeker lag at $-1/T_{seeker}$; and thus the decoupling of the nominal scheme is appreciably poor compared to the decoupling scheme (fig.3).

Due to the zero at $-RK_{sl}$; nominal scheme decoupling shows more phase lead for positive radome slope error compared to decoupling loop scheme (fig.4) while it shows more phase lag (fig.5) for negative radome slope error. This has got important repercussion for inner guidance loop stability, which would be discussed in the subsequent section.

5. Generic Stability study of Inner Guidance Loop :Nominal *vs.* Decoupling Loop Scheme:

The open loop transfer function of inner guidance loop for both nominal and decoupling loop scheme (Fig.1 and Fig.2) becomes (with Aerodynamics + Autopilot + Guidance + Noise Filter).

$$GH_{NOM} = \frac{N'V_C R}{V_m} \times \frac{\left(1+\dfrac{s}{RK_{sL}}\right)}{\left(1+\dfrac{s}{K_{sL}}\right)} \times \frac{1}{1+T_{seeker}s} \tag{11}$$

$$\times \frac{1}{1+T_{noise}s} \times \frac{1+T_\alpha s}{1+T_{ap}s} \times \frac{1}{\dfrac{s^2}{\omega_{ap}^2}+\dfrac{2\xi_{ap}}{\omega_{ap}}s+1}$$

and

$$GH_{DCP} = \frac{N'V_c R}{V_m} \times \frac{1}{\left(1+\dfrac{s}{K_{sL}}\right)(1+T_{seeker}s)} \times$$

$$\frac{1}{1+T_{noise}s} \times \frac{1+T_\alpha s}{1+T_{ap}s} \times \frac{1}{\dfrac{s^2}{\omega_{ap}^2}+\dfrac{2\xi_{ap}}{\omega_{ap}}s+1}$$

In a generic framework, a nominal 3-Loop autopilot for terminal guidance can be designed with the relationship

$T_{ap} = 0.1 \times T_\alpha$ (From transient body rate and realisability considerations),

$\omega_{ap} = 2/T_{ap}$ *to* $3/T_{ap}$ (From stability considerations) and $\xi_{ap} \approx 0.3$ to 0. (From radome slope error effect on miss distance and autopilot realisation point of view)

From equation 11 and 12, it can be seen that the variables affecting the stability of inner guidance loop are : Engagement parameters V_c/V_m (ratio of closing velocity to flight vehicle velocity), flight vehicle turning rate time constant T_α, radome error slope R, stabilisation loop gain K_{sl}, , noise filter time constant T_{noise}, autopilot dominant mode T_{ap} *and* non-dominant mode frequency ω_{ap} for a particular value of navigation constant N'. In order to establish the comparative performance evaluation / analysis of nominal scheme and decoupling loop scheme in a general framework, two types of seekers are considered with stabilization loop gain 600 and 100 which can be considered as upper and lower bounds of stabilization loop gain for practical seeker. A track loop gain of $1/T_{seeker}$ of 12 giving $T_{seeker} = 0.082$ and an equivalent track loop bandwidth of *2Hz* is considered as the type of value often employed in practical systems from tracking accuracy, RF seeker noise and guidance accuracy considerations. Also typical radome slope error in a practical system of $(R = \pm 0.02\ deg/deg)$ considered along with typical guidance parameter $N'=3$. Three types of engagement scenarios with parameters $V_c/V_m = 3, 2, 1$ are considered covering different types of flight vehicles and targets engagement generally possible. Finally, different types of flight vehicle characteristics are also incorporated for the generic studies in terms of varying guidance time constant consisting of turning rate time constant T_α, corresponding autopilot time constant and also varying noise filter time constant.

5.(a) Studies for worst type of engagement scenario i.e $V_c/V_m = 3$

For higher stabilization loop gain (say $K_{sl} = 600$); due to higher phase lead compared to nominal scheme for negative radome slope (Fig.5); decoupling scheme gives higher phase cross over frequency of inner guidance loop. But, this generally occurs at low frequency of region of interest in the rising portion of the decoupling gain curve and reduces gain margin generally marginally (fig.7). For same higher stabilization loop gain, with positive radome slope error; phase cross over frequency of nominal scheme will be higher than the decoupling scheme. However; due to somewhat lower gain attenuation of nominal scheme for higher stabilization loop gain; this effect balances out and gain margin of both schemes are close (fig.6). Thus, for higher stabilization loop gain; the performance of nominal and decoupling scheme do not vary appreciably (table-1).

For lower stabilization loop gain and with positive radome slope error; nominal scheme will have large gain amplification and will have both high gain cross over frequency and phase cross over frequency. In fact, gain cross over frequency will be higher than the phase cross over frequency (fig.8) for faster flight vehicle with low incidence lag giving unstable inner guidance loop unless noise filter time constant is substantially increased leading to considerably higher guidance time constant and thereby slowing the flight vehicle system to a great extent (fig.9, Table 1). Generally; noise filter time constant for lower bound of stabilization gain $K_{sL} = 100$ etc., should be of the order of $1/RK_{sL}$ which is high. With autopilot dominant time constant $T_{ap}=0.1*T_\propto$ generally chosen; for slower flight vehicle (say with $T_\propto = 5sec$), the autopilot lag itself considerably reduces the large gain amplification of nominal scheme due to lower stabilisation loop gain, thereby original designed noise filter time constant can be preserved and no further slowing down of guidance is required (fig.12, fig.13 & table 1). For decoupling scheme, the effect of stabilization loop gain on gain and phase characteristics of decoupling ratio is marginal (fig.3, fig.4 & fig.5) thereby giving similar stability characteristics in the decoupling scheme even with lower stabilization loop gain. As gain curve for different stabilization loop gain is sufficiently attenuated for decoupling scheme except for low frequency region; faster noise filter time constant will also yield good stability margins for faster type flight vehicle whose phase cross over frequency occurs after low frequency region and thereby a fast flight vehicle guidance system can be realized for decoupling scheme even with lower stabilization loop gain starting from fast and moderately fast flight vehicle(Fig.8). Due to absence of zero at $-RK_{sL}$; faster guidance and noise filter can be accommodated in faster type flight vehicles (i.e low T_α) (fig.9), whereas for slower flight vehicle due to high T_α and thus large amplification in the gain curve in the low frequency zone; guidance and noise filter can not be increased significantly compared to nominal scheme (Fig.14). The above findings for decoupling loop schemes are true for both positive and negative radome slope error, since the phase curve is almost same for different stabilization loop gain and gain curve is appreciably attenuated even for lower stabilization loop gain like 100.

For nominal scheme with negative radome slope error and lower stabilization loop gain, in addition to high gain amplification; normal phase cross over frequency at -180^0 is advanced to very low frequency region due to large phase lag of lower RK_{sl} and therefore phase cross over frequency at -540^0 is of importance from stability point of view giving unstable inner guidance loop (fig.10) . A high noise filter time constant is essential for faster and moderately faster type of flight vehicle system in order to sufficiently attenuate the gain curve preferably below or close to 0 dB line so as to obtain minimum required stability margin (fig.11). Thus the guidance loop becomes considerably slower with nominal scheme and lower stabilization loop gain. For appreciably slower flight vehicle (T_α = 5 sec say) and negative radome slope error ; due to low phase cross over frequency irrespective of the stabilisation loop gain variation, stability can be imparted only with higher guidance / noise filter time constant (Fig.13 & 15 and Table-1). This is true for both nominal and decoupling loop scheme and realization of faster guidance with decoupling scheme is also not feasible. Finally, it is found that almost in all the cases, the phase margin of decoupling scheme is better than the nominal scheme (table1).

5.(b) Stability performance for other engagements i.e, V_c/V_m ratio :

As engagement parameter V_c/V_m appears as a factor in inner guidance loop transfer function affecting the gain curve but not the phase (equation 11, 12) , the lower value of this parameter always improves the stability of both schemes equally. For $N^{'}V_c/V_m = 6$ and $N^{'}V_c/V_m = 3$, with same radome slope error value {+0.02 & -0.02) and stabilization gain *(* $K_{sl}=600$ *&* $K_{sl}=100$*)* as in section 5(a); i.e for $N^{'}V_c/V_m = 9$, the stability study of inner guidance loop is carried out for both nominal and decoupling loop scheme. The results are tabulated in Table 2 & Table 3 for different types of flight vehicle characteristics covering slow i.e, $T_\alpha=5\ s$ to fast flight vehicle, i.e, $T_\alpha=1\ s$. It is seen from table 1, table 2 and table 3 that for same seeker and flight vehicle characteristics , the stability characteristics are far superior and the guidance loop can be made faster for both the schemes as V_c/V_m reduces. Although this fact is well known, but the advantage of decoupling loop scheme for lower stabilization loop gain and faster type flight vehicle is brought out here even with different V_c/V_m ratio as is evident from table 2 and table 3. A considerable improvement in guidance time constant is always found achievable with decoupling scheme, even for appreciably lower stabilization loop gain like 100 and for fast and moderately faster type flight vehicles irrespective of engagement situations, i.e different V_c/V_m ratio. However, for slow flight vehicles, with decoupling loop, it is not possible to realize faster guidance. With V_c/V_m becoming lower, stability characteristics improves uniformly for both nominal and decoupling scheme and the guidance can absorb higher radome slope error. Here also, since for faster type flight vehicle, stability of decoupling is appreciably better, both faster guidance can be achieved and radome slope error can be absorbed in decoupling scheme, thereby improving performance and hardware cost / realization aspects.

6. Conclusion :

In this paper, analysis and comparative performance evaluation of two scheme namely nominal and decoupling loop scheme is addressed from the point of view of body rate attenuation in synthesized sight line rate signal, inner guidance loop stability and guidance time constant achievable for RF seeker based guided flight vehicles. Generic derivation of decoupling for both the schemes are obtained with radome aberration error. It has been brought out that for seeker with lower stabilization gain, decoupling loop scheme gives appreciable performance improvement over nominal scheme from body rate decoupling point of view, although this advantage diminishes for higher stabilization loop gain over the flight vehicle body rate frequency range generally realized. Therefore, with accurate guidance signal; better guidance performance is generally achieved in decoupling scheme.

Regarding inner guidance loop stability, it can be said in a generic framework covering different types of flight vehicles, type of engagement i.e, V_c/V_m ratio, that both schemes give similar stability characteristics for higher stabilization loop gain and different radome slope errors. Whereas for lower stabilization loop gain and for fast and moderately faster flight vehicles, decoupling scheme gives appreciably better stability characteristics with respect to nominal scheme and therefore faster guidance can be realized starting from fast and moderately fast flight vehicles covering different types of engagement . However for slower flight vehicles; faster guidance can not be realized even with decoupling scheme and stability characteristics of both the schemes are similar and dominated by radome slope error. Again; the above statement is true for different types of engagements. With V_c/V_m becoming lower, stability characteristics improves uniformly for both nominal and decoupling scheme and the guidance can absorb higher radome slope error. Here also, since for faster type flight vehicle, stability of decoupling is appreciably better, both faster guidance can be achieved and radome slope error can be absorbed in decoupling scheme, thereby improving performance and hardware cost / realization aspects.

7. References :

1. *Nesline, F.W and Zarchan P., "Missile Guidance Design Tradeoffs for High Altitude Air Defense", AIAA J. Guidance and Control, vol. 6, May - June, 1983, pp. 207 – 212.*
2. *Bhattacharjee, R.N, Rao, T.V., Sadhu, S., Ghoshal, T.K., "Control Structures and Properties of Missile Seekers", Journal of The Institute of Engineers (India), vol-82, pp 253-261, Mar-2002.*
3. *Nesline, F.W and Zarchan P., Line-of-Sight Reconstruction for faster Homing Guidance", AIAA J. Guidance and Control, vol. 8, no. 1, January – February, 1985, pp. 71 – 78*

Table-1

$R(^0/_0)$	$T_{noise}(s)$	Scheme	GM(dB)	PM(deg)	PCF(r/s)	GCF(r/s)	T_g (s)
Table-1a $N'V_c/V_m=9$, $K_{sl}=600$, $T_\alpha=1$, $T_{ap}=0.1*T_\alpha$, $\omega_{ap}=3/T_{ap}$							
+0.02	0.10	Nominal	7.1855	116.325	36.447	16.36	0.3087
		Decoupling	8.6039	∞	24.918	-	
-0.02	0.14	Nominal	6.088	∞	2.987	-	0.3487
		Decoupling	4.754	∞	4.088	-	
	0.19	Nominal	7.329	∞	2.603	-	0.3987
		Decoupling	6.0798	∞	3.456	-	
Table-1b $N'V_c/V_m=9$, $K_{sl}=600$, $T_\alpha=5$, $T_{ap}=0.1*T_\alpha$, $\omega_{ap}=3/T_{ap}$							
+0.02	0.35	Nominal	6.0339	49.712	7.761	5.74	1.0653
		Decoupling	3.1476	42.627	6.47	5.22	
	0.57	Nominal	8.5	∞	7.344	-	1.285
		Decoupling	6.019	∞	6.189	-	
-0.02	1.2	Nominal	6.3722	∞	0.744	-	1.9153
		Decoupling	5.973	∞	0.8047	-	
Table-1c $N'V_c/V_m=9$, $K_{sl}=100$, $T_\alpha=1$, $T_{ap}=0.1*T_\alpha$, $\omega_{ap}=3/T_{ap}$							
+0.02	0.7	Nominal	6.33	∞	33.484	-	0.9087
		Decoupling	22.68	∞	20.57	-	
	0.1	Nominal	-8.51	-45.52	36.05	48.8	0.3087
		Decoupling	8.04	∞	23.41	-	
-0.02	0.6	Nominal	5.92	∞	34.91	-	0.8087
		Decoupling	13.01	∞	1.15	-	
	0.2	Nominal	-2.80	-18.14	35.95	39.94	0.4087
		Decoupling	6.46	∞	3.25	-	
Table-1d $N'V_c/V_m=9$, $K_{sl}=100$, $T_\alpha=5$, $T_{ap}=0.1*T_\alpha$, $\omega_{ap}=3/T_{ap}$							
+0.02	0.6	Nominal	5.91	30.15	10.29	7.95	1.315
		Decoupling	6.06	∞	6.07	-	
-0.02	0.95	Nominal	6.1117	100.68	0.6133	0.2313	1.6653
		Decoupling	4.6345	∞	0.9173	-	
	1.20	Nominal	7.38	∞	0.54	-	1.9135
		Decoupling	6.00	∞	0.79	-	

Table-2

$R(^0/^0)$	$T_{noise}(s)$	Scheme	GM(dB)	PM(deg)	PCF(r/s)	GCF(r/s)	T_g (s)
$N'V_c/V_m$=6, K_{sl}=600, T_α=1, T_{ap}=0.1* T Table-2a $_\alpha$, ω_{ap}=3/ T_{ap}							
+0.02	0.10	Nominal	10.707	∞	36.47	-	0.3087
		Decoupling	12.126	∞	24.917	-	
-0.02	0.10	Nominal	8.482	∞	3.3771	-	0.3087
		Decoupling	7.068	∞	4.6023	-	
Table-2b $N'V_c/V_m$=6, K_{sl}=600, T_α=5, T_{ap}=0.1* T_α, ω_{ap}=3/ T_{ap}							
+0.02	0.10	Nominal	8.72	51.2	10.17	6.87	0.8153
		Decoupling	3.946	37.68	7.719	6.33	
	0.30	Nominal	8.928	∞	7.926	-	1.0153
		Decoupling	5.9	∞	6.582	-	
-0.02	0.60	Nominal	6.27	∞	1.07	-	1.3153
		Decoupling	5.78	∞	1.17	-	
Table-2c $N'V_c/V_m$=6, K_{sl}=100, T_α=1, T_{ap}=0.1* T_α, ω_{ap}=3/ T_{ap}							
+0.02	0.4	Nominal	6.194	∞	33.73	-	0.6087
		Decoupling	22.562	∞	20.88	-	
	0.1	Nominal	-4.99	-29.94	36.05	43.31	0.3087
		Decoupling	11.56	∞	23.41	-	
-0.02	0.4	Nominal	6.098	∞	35.157	-	0.6087
		Decoupling	13.846	∞	1.994	-	
	0.1	Nominal	-4.024	-24.09	37.45	43.33	0.3087
		Decoupling	7.245	∞	4.434	-	
Table-2d $N'V_c/V_m$=6, K_{sl}=100, T_α=5, T_{ap}=0.1* T_α, ω_{ap}=3/ T_{ap}							
+0.02	0.33	Nominal	6.169	30.987	11.072	8.42	1.0453
		Decoupling	6.093	∞	6.414	-	
-0.02	0.4	Nominal	5.98	69.61	0.871	7.742	1.1153
		Decoupling	4.146	∞	1.38	-	
	0.6	Nominal	7.478	100.9	0.756	6.385	1.3153
		Decoupling	5.821	∞	1.16	-	

Table-3

$R(^0/^0)$	$T_{noise}(s)$	Scheme	GM(dB)	PM(deg)	PCF(r/s)	GCF(r/s)	T_g (s)
Table-3a $N'V_c/V_m$=3, K_{sl}=600, T_α=1, T_{ap}=0.1* T_α, ω_{ap}=3/ T_{ap}							
+0.02	0.10	Nominal	16.728	∞	36.44	-	0.3087
		Decoupling	18.146	∞	24.917	-	
-0.02	0.10	Nominal	14.502	∞	3.377	-	0.3087
		Decoupling	13.09	∞	4.602	-	

Table-3 contd..							
Table-3b ***$N'V_c/V_m$=3, K_{sl}=600, T_α=5, T_{ap}=0.1* T_α, ω_{ap}=3/ T_{ap}***							
+0.02	0.10	Nominal	14.74	∞	10.17	-	0.8153
		Decoupling	9.966	∞	7.72	-	
-0.02	0.10	Nominal	7.6565	∞	1.7976	-	0.8153
		Decoupling	6.911	∞	2.0545	-	
Table-3c ***$N'V_c/V_m$=3, K_{sl}=100, T_α=1, T_{ap}=0.1* T_α, ω_{ap}=3/ T_{ap}***							
+0.02	0.206	Nominal	6.00	∞	34.51	-	0.4147
		Decoupling	22.472	∞	21.87	-	
	0.1	Nominal	1.031	8.094	36.049	34.525	0.3087
		Decoupling	17.586	∞	23.414	-	
-0.02	0.181	Nominal	6.00	84.1	36.11	23.82	0.3897
		Decoupling	15.53	∞	3.4308	-	
	0.1	Nominal	2.00	15.55	37.453	34.52	0.3087
		Decoupling	13.267	∞	4.434	-	
Table-3d ***$N'V_c/V_m$=3, K_{sl}=100, T_α=5, T_{ap}=0.1* T_α, ω_{ap}=3/ T_{ap}***							
+0.02	0.1	Nominal	9.6	52.72	14.47	8.93	0.8153
		Decoupling	9.51	∞	7.56	-	
-0.02	0.1	Nominal	9.238	81.11	1.14	8.825	0.8153
		Decoupling	6.986	∞	2.024	-	

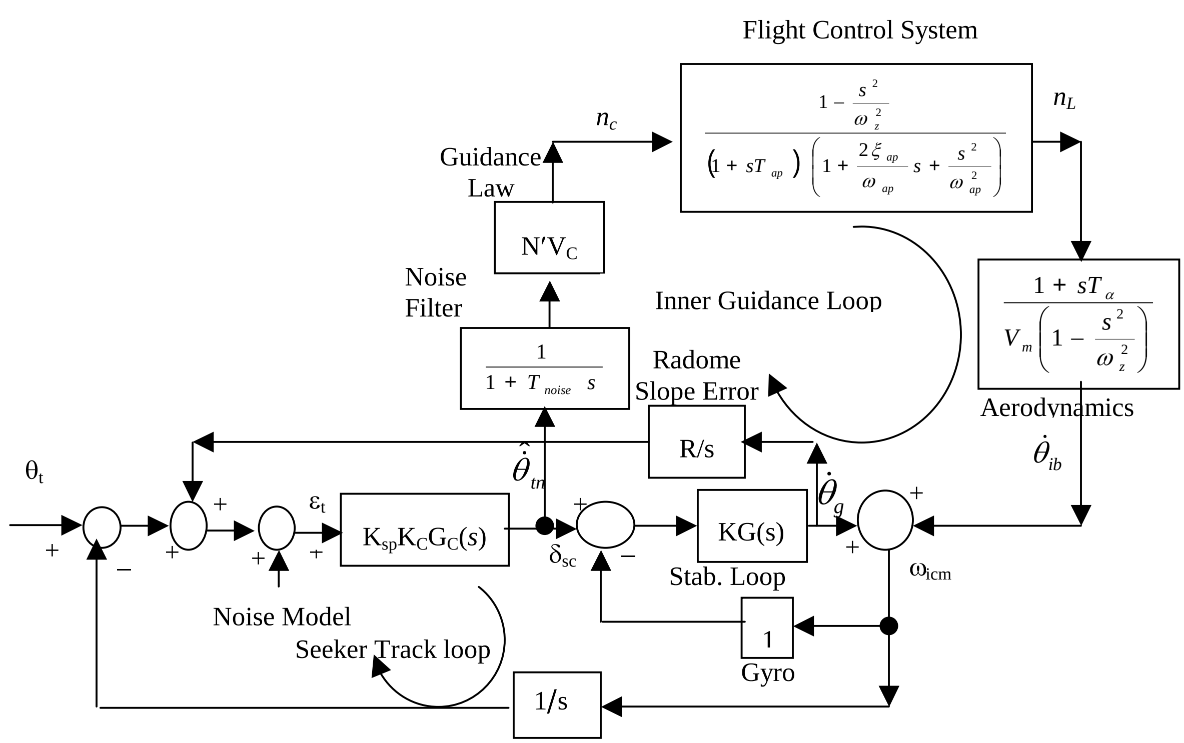

Figure-1 Inner Guidance Loop with Nominal Scheme

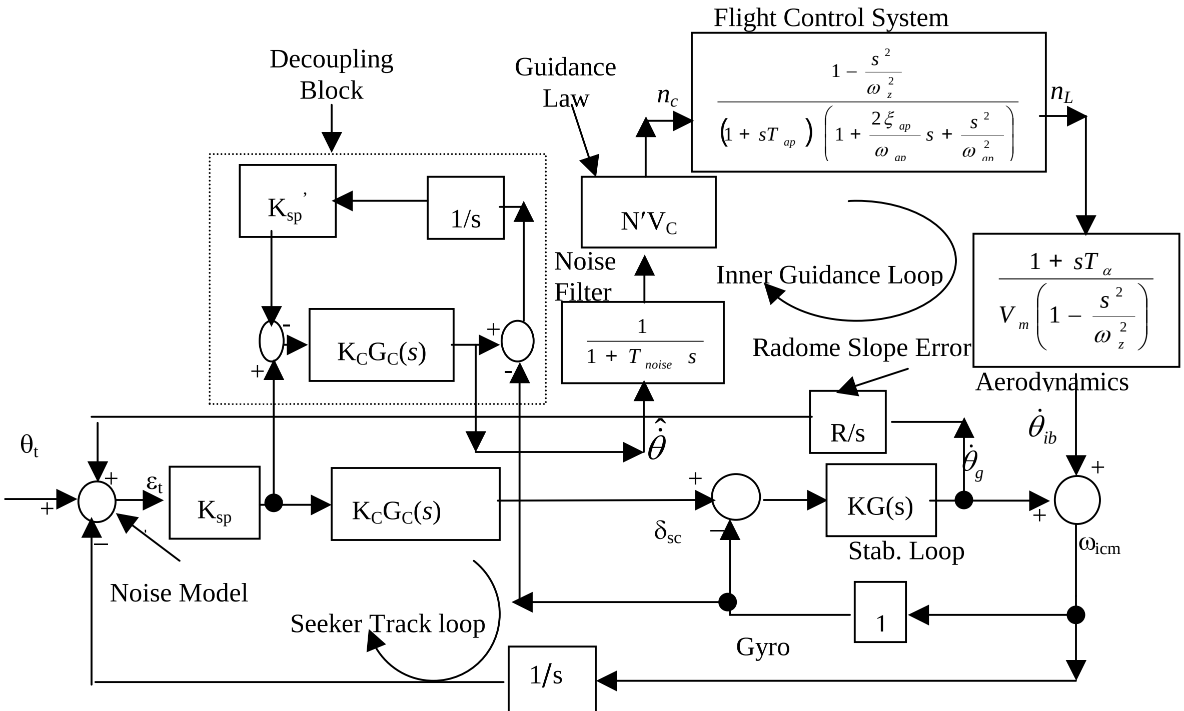

Fig.2 Inner Guidance Loop with Decoupling Loop Scheme

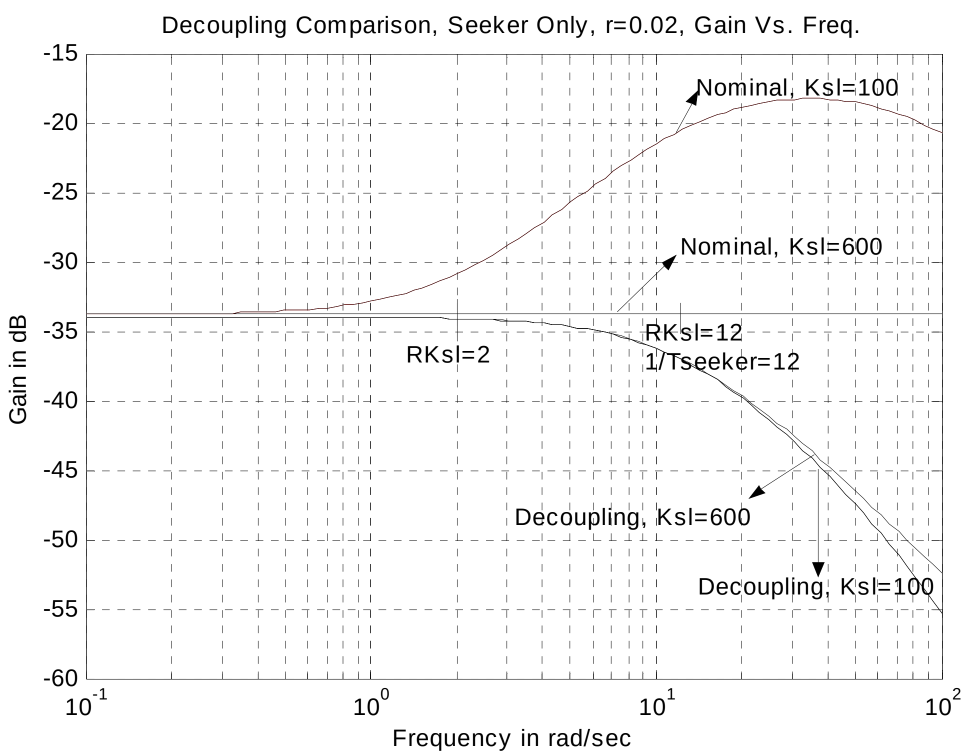

Figure-3

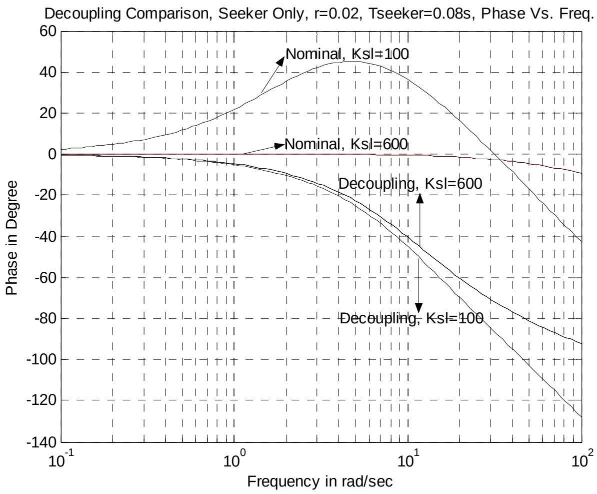

Figure-4

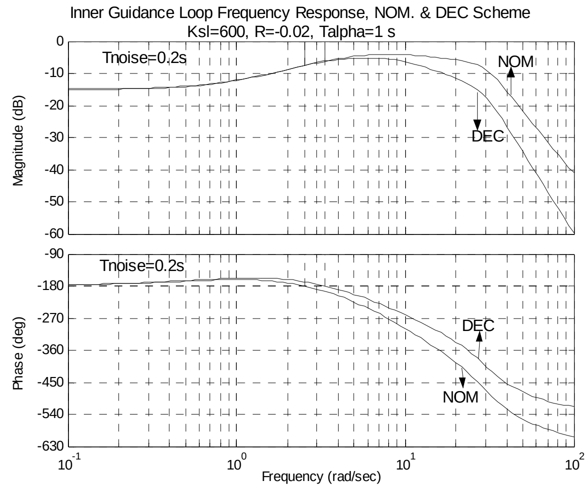

Figure-7

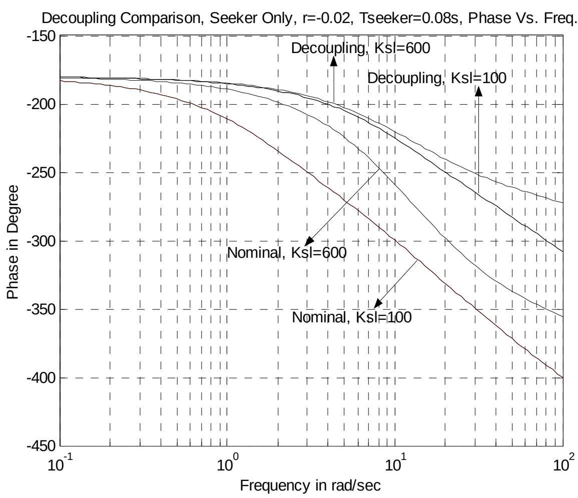

Figure-5

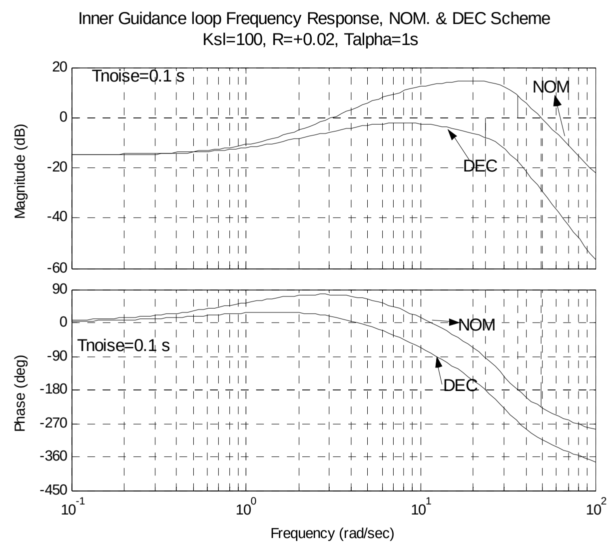

Figure-8

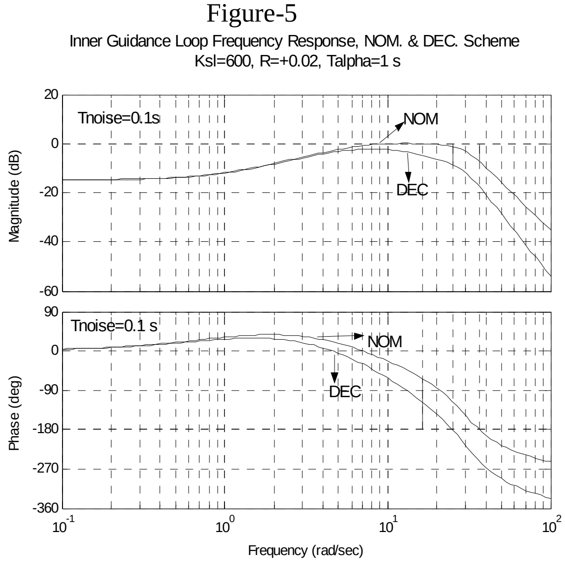

Figure-6

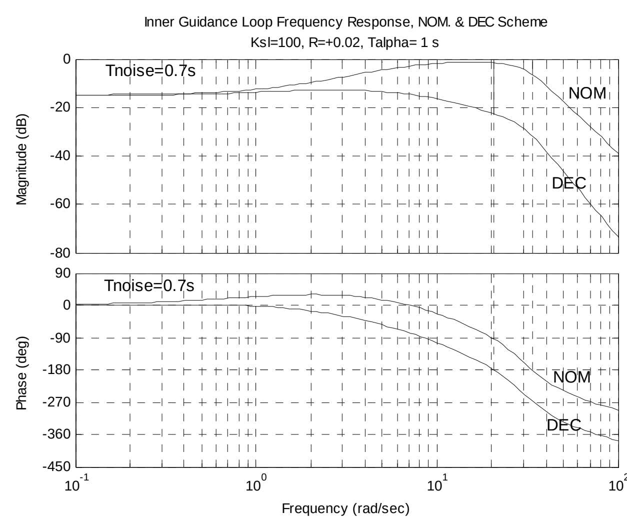

Figure-9

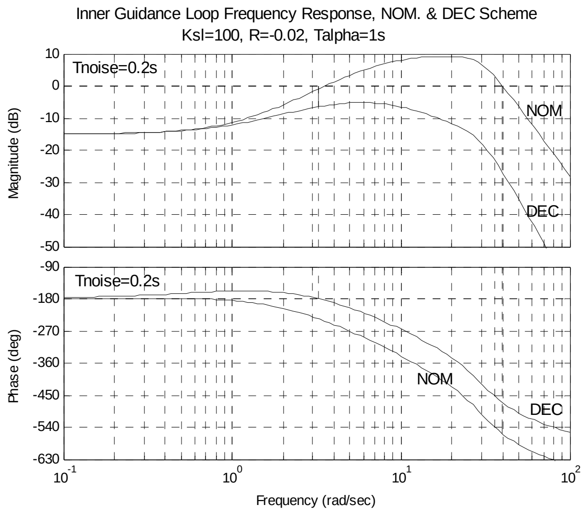

Figure-10

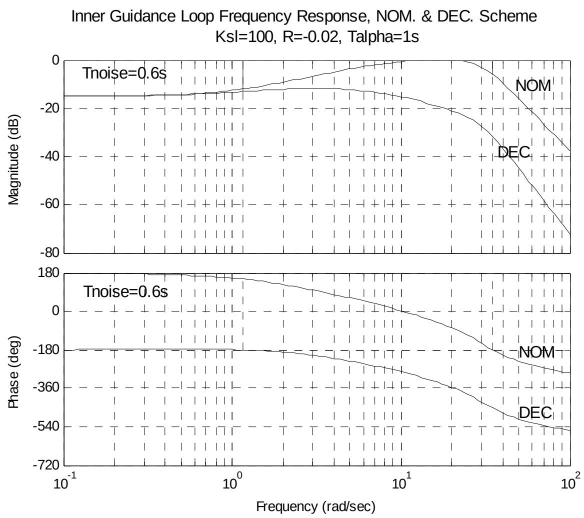

Figure-11

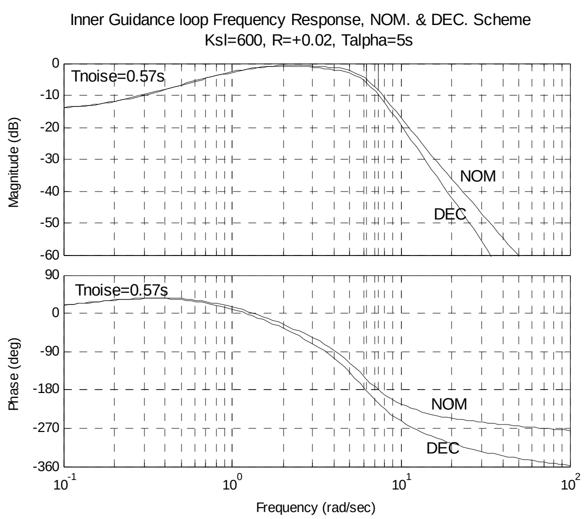

Figure-12

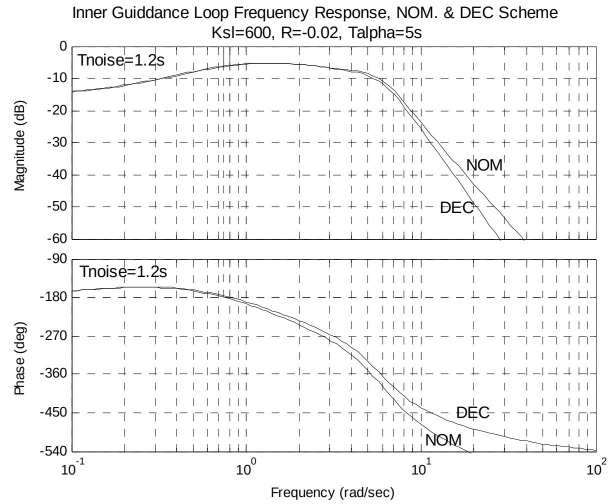

Figure-13

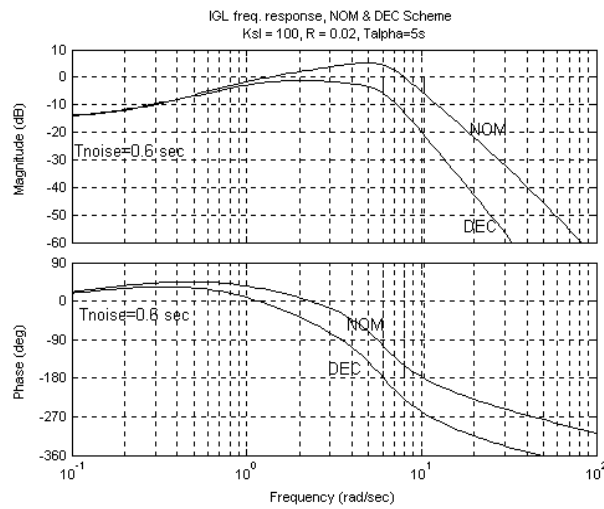

Figure-14

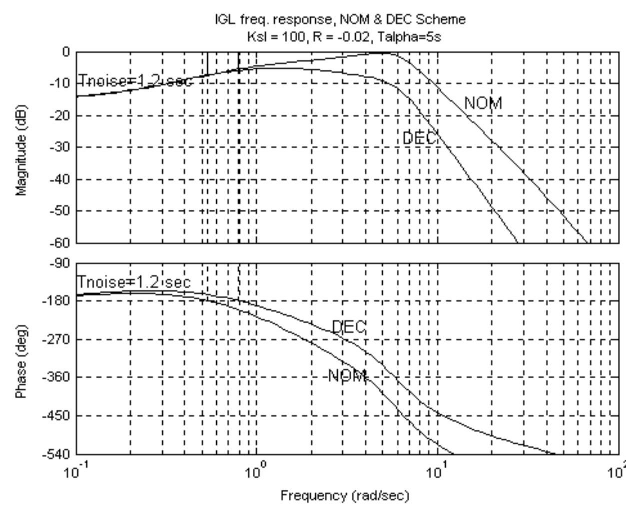

Figure-15